ELSEVIER

International Journal of Thermal Sciences 41 (2002) 753–762

International Journal of Thermal Sciences

www.elsevier.com/locate/ijts

Dynamic modeling of the combined heat and mass transfer during the adsorption/desorption of water vapor into/from a zeolite layer of an adsorption heat pump

Thorsten Miltkau, Belal Dawoud *

Institute of Technical Thermodynamics, Aachen University of Technology (RWTH Aachen), Schinkelstr. 8, D-52056 Aachen, Germany

Received 23 March 2001; accepted 20 September 2001

Abstract

This paper presents a one-dimensional model describing the combined heat and mass transfer during the adsorption/desorption of water vapor into/from a zeolite layer in a small-scale adsorption heat pump. The model is utilized to study the dynamics of both adsorption and desorption processes as well as to examine the influence of both the layer thickness and the volume of the vapor phase of the adsorber/desorber heat exchanger on their time requirements. The model equations have been numerically solved using the software packet gPROMS (**g**eneral **PRO**cess **M**odeling **S**ystem) [http://www.psenterprise.com/gPROMS]. The duration of the adsorption process is found to be generally longer than that of the desorption process, depending on the zeolite layer thickness. Reducing the layer thickness by 50% results in a reduction to 25% in the duration of the adsorption process and to about 33% of the desorption process. In order to get reasonable power densities from an adsorption heat pump using zeolite layers, the layer thickness must not exceed 2.5 mm. Moreover, the volume of the vapor phase of the adsorber/desorber heat exchanger has to be minimized, in order to minimize the unavoidable losses of the coefficient of performance of the periodical adsorption heat pump due to the pre-cooling as well as the pre-heating phases.

Keywords: Adsorption heat pump; Dynamic modeling; gPROMS; Heat and mass transfer; Zeolite–water; Zeolite layer

1. Introduction

Adsorption-based technologies hold the potential for replacing chlorofluorocarbon (CFC)-based refrigeration and heat pump systems, thereby replacing ozone-depleting working fluids. One of the most interesting working pairs for adsorption heat pumps (AHPs) is zeolite–water. This working pair is non-poisonous, non-flammable and, moreover, has no ozone depletion potential.

The adsorption of water vapor into a porous solid adsorbent, such as zeolite, results in the release of the heat of adsorption. Accordingly, the temperature of the adsorbent particle rises, which reduces its adsorptive capacity. Therefore, the heat of adsorption has to be removed before a further vapor mass transfer into the adsorbent may take place. Thus, the rate of vapor adsorption in zeolite is mainly controlled by both heat and mass transfer mechanisms within the zeolite bed [2,3]. The evaluation of the heat and mass transfer rates accompanied with such an adsorption process is, therefore, very important in designing and optimizing the operation of an adsorption heat pump.

Zeolite can be utilized in different forms in designing the adsorber/deorber heat exchanger of an AHP. Making use of zeolite in the form of powder is unfavorable since the coupled heat and mass transfer inside a pulverized zeolite bed is insufficient [4]. Investigations carried out on adsorption beds using zeolite pellets [5–7] showed that the initial adsorption rate is high due to the large surface area of the zeolite bed. However, the poor thermal conductivity of zeolite beds (0.15 $W \cdot m^{-1} \cdot K^{-1}$ [8]) and the poor contact between the zeolite pellets and the heat exchanger wall results in a steep drop in the adsorption rate. This leads to long cycle times and, consequently, to a low thermal output of the heat pump.

Alternatively, zeolite layers could be linked directly to the heat transfer area, resulting in higher thermal conductivities than zeolite beds. One disadvantage of these layers is the smaller mass transfer area compared to granules. The low

* Correspondence and reprints.
E-mail address: dawoud@ltt.rwth-aachen.de (B. Dawoud).

1290-0729/02/$ – see front matter
PII: S1290-0729(02)01369-8

Nomenclature

a_1–a_6	parameters of Eq. (10)	
A	cross-sectional area of the zeolite layer	m^2
A_{MaP}	cross-sectional area of macropores	m^2
d_{MaP}	diameter of macropores	m
D_{geo}	geometrical diffusion parameter	m
D_{Kn}	Knudsen diffusion coefficient	s
h	enthalpy	$KJ{\cdot}kg^{-1}$
Kn	Knudsen number	
$\dot{m}$	mass flow rate	$kg{\cdot}s^{-1}$
$\dot{m}''$	mass flux (mass flow rate per unit area)	$kg{\cdot}s^{-1}{\cdot}m^{-2}$
M_g	molecular weight of gas	$kg{\cdot}kmol^{-1}$
P	pressure	mbar
R_m	universal gas constant	$kJ{\cdot}kmol^{-1}{\cdot}K^{-1}$
S	thickness of zeolite layer	m
t	time	s
T	temperature	K
u	specific internal energy	$kJ{\cdot}kg^{-1}$
V	volume	m^3
x	water uptake	
Z	spatial coordinate	m

Greek symbols

α	heat transfer coefficient	$W{\cdot}m^{-2}{\cdot}K^{-1}$
ϕ	relative humidity of zeolite	
λ	thermal conductivity of zeolite layer	$W{\cdot}m^{-1}{\cdot}K^{-1}$
Λ_g	free length of path	m
ρ	density of loaded zeolite	$kg{\cdot}m^{-3}$
μ_{MaP}	tortuosity factor	
ψ_{MaP}	porosity of zeolite	
χ	relative water uptake	

Subscripts

ave	average value
c	crystal
MaP	macropore
O	initial value
∞	final value
v	vapor
W	wall
Z	spatial coordinate
zeo, dry	dry zeolite

diffusivity of the solid may dominate the adsorption process [9].

It is, therefore, the aim of this work to clarify these questions by investigating the combined heat and mass transfer during the adsorption/desorption of water vapor into/from a zeolite layer. Moreover, the presented simulation model is used to examine the influence of both the zeolite layer thickness and the volume of the vapor phase of the adsorber/desorber heat exchanger on the dynamics of a small-scale zeolite–water AHP.

2. The considered adsorption heat pump

Adsorption heat pumps can be built up with a various number of heat exchangers. As a central component of the adsorption heat pump, the adsorber determines the operating characteristics of the heat pump with regard to both energetic process quality and attainable power density. The considered heat pump consists of the components condenser, evaporator, adsorber/desorber and their connecting piping. In the vapor piping, non-return valves have been integrated. During the adsorption phase, depicted in Fig. 1, the adsorber heat transfer medium (AdHTM) connects the heating net to the adsorber heat exchanger (AdHEX). The pressure decreases and the refrigerant vapor flows from the evaporator to the adsorber through the evaporator non-return valve.

During the desorption phase, both switching valves S have to be reswitched to connect the AdHEX with the burner. In this high pressure phase, the evaporator non-return valve is closed and the condenser non-return valve is opened to connect the desorber with the condenser.

Condenser and evaporator are connected to each other through a throttling valve, which, during the adsorption phase, supplies the evaporator with the refrigerant stored in the condenser. Consequently, the evaporator can be designed as a falling film evaporator. This throttling valve has to be closed during the desorption phase.

3. Mathematical model

In this section, the set of equations describing the model of the combined heat and mass transfer in a zeolite layer will be illustrated. Fig. 2 shows the discretisation of the zeolite layer. The following basic assumptions were made:

(1) The heat and mass transfer problem is considered to be one-dimensional.
(2) All infinitesimally small zeolite sub-layers are considered to be phases in thermodynamic equilibrium.
(3) The heat content within the vapor phase can be neglected for the density ratio between vapor and liquid phase is very small. At the working temperature and pressure of 100 °C and 100 mbar respectively, for example, the density ratio between vapor and liquid is approximately 5.0×10^{-5}.
(4) The zeolite layer and the adsorbed water are considered to be incompressible.

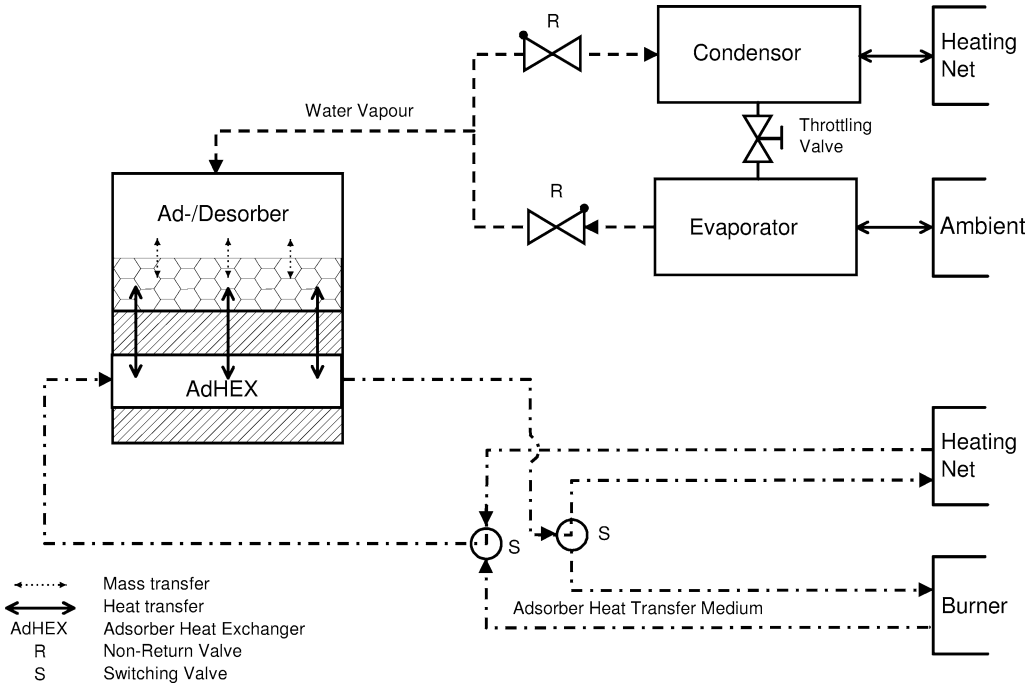

Fig. 1. Schematic presentation of the considered adsorption heat pump.

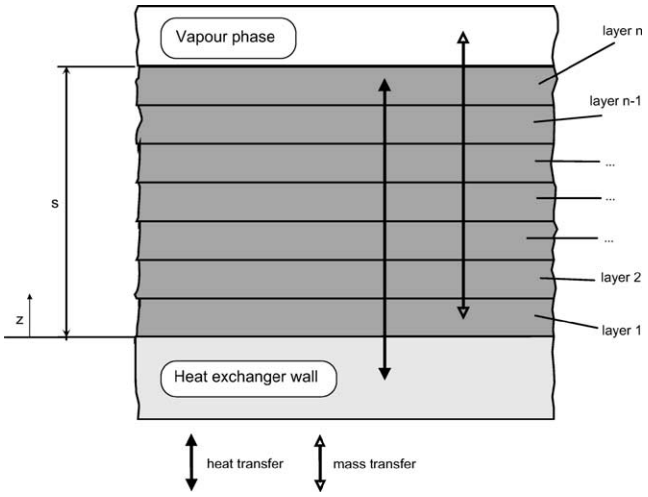

Fig. 2. Discretisation of the zeolite layer.

(5) The mass transfer within the zeolite layer is determined by the macropore diffusion of water vapor.

3.1. Energy balance

The energy balance for the zeolite layer, including the diffusive enthalpy rate of the absorbed vapor, can be formulated as follows [10]:

$$\frac{\partial}{\partial t}\big(\rho(x)\cdot u(x,T)\big) = \frac{\partial}{\partial z}\left(\lambda\cdot\frac{\partial T}{\partial z}\right) - \frac{\partial}{\partial z}\big(\dot{m}''_{\mathrm{v}}\cdot h_{\mathrm{v}}\big) \qquad (1)$$

Where $u(x,T)$ represents the specific internal energy of wetted zeolite, which is a function of both the water uptake x and the prevailing zeolite temperature T, and $\dot{m}''_{\mathrm{v}}$ is the mass flux of the adsorbed water vapor. The temperature dependence of the internal energy is expressed in terms of the specific heat capacity of water loaded zeolite, while the uptake dependence is represented by the partial differential internal energy of the adsorbed water [11]. The partial differential internal energy is, in turn, defined, for an incompressible adsorption system, as the difference between the enthalpy of water vapor and the differential isosteric heat of adsorption.

3.2. Mass balance

The continuity equation for each sub-layer can be formulated as follows [12]:

$$\frac{\partial\rho}{\partial t} = -\frac{\partial\dot{m}''_{\mathrm{v}}}{\partial z} \qquad (2)$$

3.3. Mass transfer

Depending on the prevailing pressure and temperature and the diameter of the macropores, the mass transfer of water vapor into the pores of zeolite is influenced by various mechanisms [3]. The dominating mechanism can be estimated from the Knudsen number Kn which describes the ratio of the free length of path Λ_{g} of gas molecules to the diameter of the macropores d_{MaP} and is given by:

$$Kn = \frac{\Lambda_{\mathrm{g}}}{d_{\mathrm{MaP}}} \qquad (3)$$

The share of free mass flow exceeds that of Brownian movement of the vapor molecules (Knudsen Diffusion) if

the Knudsen number is less than 0.1 [3]. With a diameter of the macropores of around 600 nm and typical working pressures and temperatures of a zeolite–water heat pump, the Knudsen number is always greater than 0.5. This implies that the dominating mechanism of mass transfer of water vapor in the zeolite structures is the Brownian movement.

From the kinetic gas theory, the mass transfer rate of water vapor through the macropores can be expressed, according to [12–14], as:

$$\dot{m}_{\mathrm{v}} = A_{\mathrm{MaP}} \cdot \frac{D_{Kn}}{\mu_{\mathrm{MaP}}} \cdot \frac{\partial p}{\partial z} \tag{4}$$

with

$$A_{\mathrm{MaP}} = A \cdot \psi_{\mathrm{MaP}} \tag{5}$$

and

$$D_{Kn} = \frac{4}{3} \cdot d_{\mathrm{MaP}} \cdot \sqrt{\frac{M_{\mathrm{g}}}{2 \cdot \pi \cdot R_{\mathrm{m}} \cdot T}} \tag{6}$$

The mass transfer rate is directly proportional to the pressure gradients in the z direction, the cross-sectional area of the macropores A_{MaP}, the diffusion coefficient D_{Kn} and inversely proportional to the tortuosity (or labyrinth) factor μ_{MaP} which depends on the pore structure of the zeolite. The Knudsen diffusion coefficient D_{Kn} is described in terms of the diameter of the macropores d_{MaP} and the Brownian movement of the vapor molecules. In Eq. (7), the porosity of the zeolite particles ψ_{MaP}, the diameter of the macropores and the tortuosity factor are combined to give the geometrical diffusion parameter D_{geo}:

$$D_{\mathrm{geo}} = \frac{\psi_{\mathrm{MaP}} \cdot d_{\mathrm{MaP}}}{\mu_{\mathrm{MaP}}} \tag{7}$$

A geometrical diffusion parameter of 3.0×10^{-7} m is obtained for $d_{\mathrm{MaP}} = 600$ nm, $\psi_{\mathrm{MaP}} = 0.5$, and $\mu_{\mathrm{MaP}} = 1.0$ [3].

Combining Eqs. (4)–(7), the mass fluxes of adsorbate can be expressed as:

$$\dot{m}''_{\mathrm{v}} = \frac{\dot{m}_{\mathrm{v}}}{A} = D_{\mathrm{geo}} \cdot \frac{4}{3} \cdot \sqrt{\frac{M_{\mathrm{g}}}{2 \cdot \pi \cdot R_{\mathrm{m}} \cdot T}} \cdot \frac{\partial p}{\partial z} \tag{8}$$

3.4. Heat transfer

The heat transfer within the zeolite layer is expressed in terms of the effective thermal conductivity λ which takes into account the porosity of the zeolite particles ψ_{MaP}.

$$\lambda = \lambda_{\mathrm{c}} \cdot (1 - \psi_{\mathrm{MaP}}) \tag{9}$$

where the thermal conductivity of the zeolite crystal $\lambda_{\mathrm{c}} = 0.58\ \mathrm{W{\cdot}m^{-1}{\cdot}K^{-1}}$ [3].

3.5. Adsorption equilibrium data

According the second assumption, all infinitesimally small zeolite sub-layers are considered to be phases in thermodynamic equilibrium. The adsorption equilibrium data of the considered adsorbent/adsorbate pair (zeolite–MgNaA/water) are described by the following isotherm equation, developed by Dawoud [11].

$$\frac{x}{a_1} = a_2 \cdot \frac{[(a_3/\sqrt{T})\exp(a_4/T)] \cdot p}{1 + [(a_3/\sqrt{T})\exp(a_4/T)] \cdot p} + (1 - a_2) \cdot \frac{\{[(a_5/\sqrt{T})\exp(a_6/T)] \cdot p\}^2}{1 + \{[(a_5/\sqrt{T})\exp(a_6/T)] \cdot p\}^2} \tag{10}$$

The parameters of this equation are given in Table 1, according the range of the relative humidity of zeolite ϕ, which is defined as the ratio between the equilibrium vapor pressure of the adsorbed water p and the saturation vapor pressure of water at the zeolite temperature T.

3.6. Density

Neglecting the volume of the adsorbed water in zeolite, the density of the water loaded zeolite can be expressed as follows;

$$\rho = \rho_{\mathrm{zeo,dry}} \cdot (1 + x) \tag{11}$$

where $\rho_{\mathrm{zeo,dry}}$ is the density of dry zeolite. It is taken to be equal 535 $\mathrm{kg{\cdot}m^{-3}}$ [15].

3.7. Relative water uptake

The relative water uptake χ defined as:

$$\chi = \frac{x_{\mathrm{ave}} - x_{\mathrm{o}}}{x_{\infty} - x_{\mathrm{o}}} \tag{12}$$

is the ratio of the time dependent quantity of the adsorbed water, per kg of dry zeolite, to the maximum possible adsorbable quantity, which is related to the operating conditions of the AHP and the adsorption equilibrium data of the considered zeolite–water system. The average water uptake x_{ave} is the integrated uptake over the zeolite layer thickness.

3.8. Conservation of mass in the vapor phase

The time rate of decrease of the mass of water vapor, in the vapor phase, is equal to the adsorbed mass flow rate of water vapor on the top of the zeolite layer.

$$\frac{\partial m_{\mathrm{v}}}{\partial t} = -\dot{m}''_{\mathrm{v}}(s) \cdot A \tag{13}$$

Table 1
Parameters of Eq. (10)

Parameter	$\phi < 0.01$	$\phi \geqslant 0.01$
a_1	0.171	0.319
a_2	0.233	0.710
a_3	1.069E–07	3.084E–08
a_4	8704.2	6901.3
a_5	5.192E–08	2.613E–10
a_6	6751.5	7171.5

3.9. Pressure estimation in the vapor phase

The ideal gas behavior is assumed for the water vapor phase.

$$p_v \cdot V_v = m_v \cdot R_v \cdot T_v \tag{14}$$

4. Boundary and initial conditions

4.1. Boundary conditions

4.1.1. Heat transfer

The heat transfer from the zeolite layer to the heat exchanger wall is assumed to take place with a wall heat transfer coefficient of $\alpha_W = 280\ \mathrm{W{\cdot}m^{-2}{\cdot}K^{-1}}$ [16].

$$-\lambda \cdot \left.\frac{\partial T}{\partial z}\right|_{Z=0} = \alpha_W \cdot (T_W - T|_{z=0}) \tag{15}$$

The energy exchange between the outer-most zeolite sublayer and the vapor phase is assumed to be purely due to the diffusive enthalpy flow of the adsorbed water vapor. In other words, the heat transfer by convection as well as radiation with the vapor phase is neglected. The relevant boundary condition to the energy equation can, thus, be formulated as:

$$\left.\frac{\partial T}{\partial z}\right|_{Z=S} = 0 \tag{16}$$

4.1.2. Mass transfer

Regarding the mass transfer within the zeolite layer, it is assumed that there is no mass transfer from the bottom of the zeolite layer. The pressure in the vapor phase is set equal to the pressure at the outermost segment of the zeolite layer.

$$\left.\frac{\partial p}{\partial z}\right|_{z=0} = 0 \tag{17}$$

$$p|_{z=s} = p_v \tag{18}$$

4.2. Initial conditions

The zeolite layer has initially a homogeneous temperature and water uptake, and accordingly, a homogeneous equilibrium vapor pressure distribution.

5. Solution method

For the very fact that periodically operating adsorption heat pumps work under transient conditions, the model equations expressed above are coordinate and time dependent. To consider the coordinate dependency, the zeolite layer is discretised into balance elements in the Z-direction (Fig. 2). The gPROMS package [1] has been used for the system modeling and simulation. The system of partial differential an algebraic equations (PDAEs) presented above is written directly in gPROMS using its high-level modeling language [17] and is then solved using the method of lines family of numerical methods. This involves the automatic discretisation of the distributed equations with respect to all spatial domains, which results in mixed sets of time-dependent ordinary differential and algebraic equations (DAEs). The resulting DAE system is then solved by gPROMS' built-in DAE solver. In this paper, among the various discretisation techniques available with gPROMS, the centered finite difference (CFDM) and the orthogonal collocation on finite element methods (OCFEM) are tested.

6. The simulated processes

The simulated adsorption process starts directly after completing a desorption/condensation phase, during which the zeolite layer reaches the homogenous equilibrium conditions given in Table 2. The vapor pressure is then equal to the condenser pressure of 85.0 mbar. Reswitching the two S-valves in Fig. 1, the AdHEX is thus connected with the heating net, and the wall temperature is assumed to have a sudden drop from 180 °C to 50 °C. This results in cooling the zeolite layer and leads to the adsorption of some water vapor and, consequently, a reduction of the vapor pressure. As soon as the vapor pressure decreases below the condenser pressure, the condenser non-return valve is closed and the adsorber works as a closed system. The further adsorption results in further decrease of the vapor pressure until it reaches the evaporator pressure. At this time, the so-called pre-cooling phase is completed, the conditions for the adsorption process under constant evaporator pressure are reached and the adsorber starts working as an open system. The adsorption process continues until the relative water uptake reaches 0.95.

The desorption process starts from the end of the adsorption phase with the starting conditions listed in Table 3. The AdHEX is to be connected to the burner and the wall

Table 2
Fixed parameters, initial and boundary conditions of the adsorption process

Mass of dry zeolite	42 g
Volume of vapor phase	10 liters
Initial uptake x_o	0.075
Initial temperature of zeolite layer	180 °C
Initial vapor pressure	85.0 mbar
Wall temperature	50 °C
Evaporator pressure	8.7 mbar

Table 3
Fixed parameters, initial and boundary conditions of the desorption process

Mass of dry zeolite	42 g
Volume of vapor phase	10 liters
Initial uptake x_o	0.227
Initial temperature of zeolite layer	50 °C
Initial vapor pressure	8.7 mbar
Wall temperature	180 °C
Condenser pressure	85.0 mbar

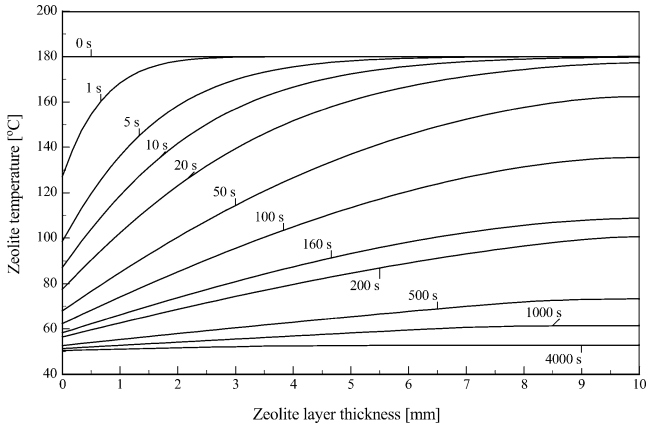

Fig. 3. Temperature distribution over the zeolite layer thickness with the time as a parameter.

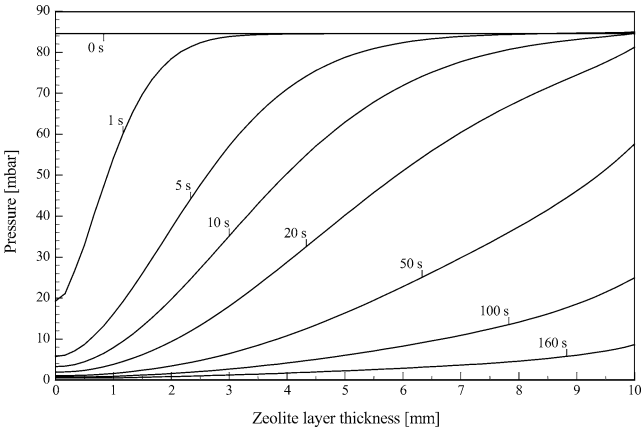

Fig. 4. Pressure distribution over the zeolite layer thickness in the first 160 seconds of the adsorption process.

temperature is assumed to have sudden change to 180 °C, which results in desorbing some water vapor from zeolite layer and, consequently, increasing the vapor pressure. At this moment, the evaporator non-return valve is closed and the desorber works as a closed system until the vapor pressure reaches the condenser pressure. At this time, the so-called pre-heating phase is completed. The condenser is assumed to be designed to hold the vapor pressure at a constant level of 85.0 mbar during the rest of the desorption process, which then continues until the relative water uptake reaches 0.05.

The volume of the vapor phase of the adsorber/desorber heat exchanger is taken to be 10 liter. This is quite high for the considered mass of 42 g of zeolite. However, the effect of this volume on the duration of pre-cooling, adsorption, pre-heating and desorption phases will also be investigated in detail.

7. Results

7.1. Degree of discretisation and discretisation methods

The discretisation methods along with the degree of discretisation have been tested on an adsorption process having the initial and boundary conditions listed in Table 2. For a zeolite layer thickness of 10 mm, a minimum grid of 40 intervals or elements was required for CFDM and OCFEM, respectively, to give identical courses of time variations in pressure, temperature and water uptake. A grid of twenty five intervals or elements was required for a layer thickness of 5 mm. However, the discretisation with the OCFEM requires 160% as much CPU-time as that required for the same problem when discretised with CFDM. Therefore, the CFDM is applied through the rest of this work.

7.2. Adsorption process

7.2.1. Temperature distribution

The variation of zeolite temperature over the zeolite layer thickness at some selected time instants, for a zeolite layer of 10 mm thickness being discretised in 60 intervals using CFDM, is shown in Fig. 3. The temperature of the lower-most zeolite sub-layer decreases sharply in the first second to 128 °C, while that of the outer-most sub-layer starts to decrease after 10 s. The temperature distribution reaches nearly its steady state after 4000 s.

7.2.2. Pressure and uptake distributions

Fig. 4 shows the pressure distribution over the zeolite layer thickness in the first 160 s of the adsorption process. At the bottom of the zeolite layer and due to the sharp decrease in temperature, within the first second shown in Fig. 3, the vapor pressure decreases sharply to 20 mbar. This decrease in pressure is faster than that in temperature due to the exponential dependence of the equilibrium vapor pressure on the zeolite temperature at a constant water uptake [11]. As the temperature wave reaches the top of the layer after 10 s, the pressure starts to decrease from there on. After 160 s, the pre-cooling phase is terminated, and the vapor pressure at the outer-most sub-layer reaches the evaporator pressure of 8.7 mbar. This pressure is assumed to be held constant, due to a proper evaporator design, for the rest of the adsorption process. Fig. 5 shows the uptake distribution over the zeolite layer for the first 200 s of the adsorption process. It can be seen that the variation in the uptake distribution within the first 10 s of the adsorption process is purely a redistribution of the adsorbed water within the zeolite layer. Due to the resulting high pressure gradient (see Fig. 4) from the high temperature gradient (see Fig. 3) near the wall of the heat exchanger, the water adsorbed around the middle of the layer moves towards the wall. This explains the rapid increase of the uptake near the wall in the first 100 s. This, in turn, results in a negative pressure gradient and consequently in a new redistribution of the adsorbed water. The negative pressure

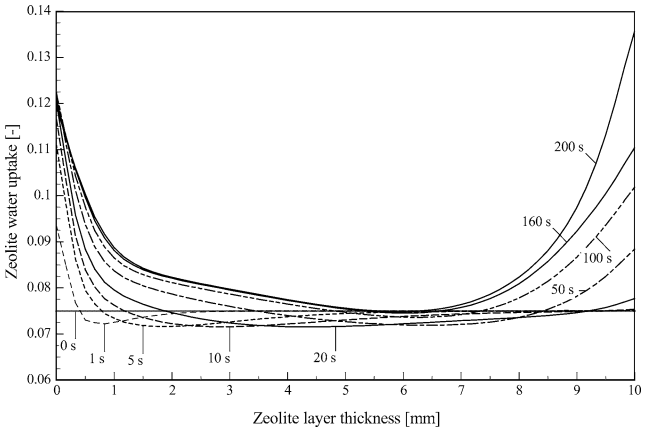

Fig. 5. Uptake distribution over the zeolite layer thickness in the first 200 s of the adsorption process.

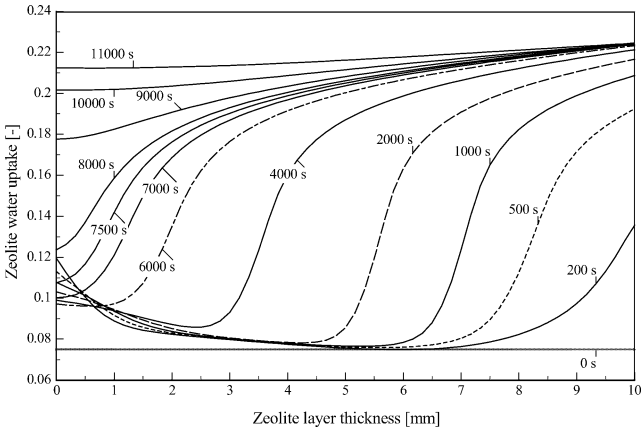

Fig. 7. Uptake distribution over the zeolite layer thickness after the first 200 s of the adsorption process.

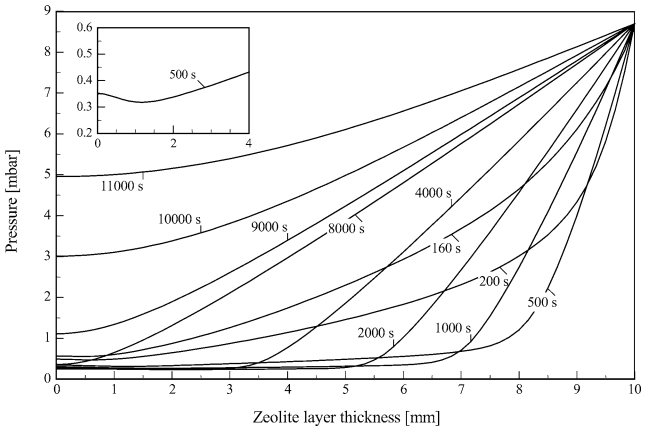

Fig. 6. Pressure distribution over the zeolite layer thickness after 160 s from the beginning of the adsorption process.

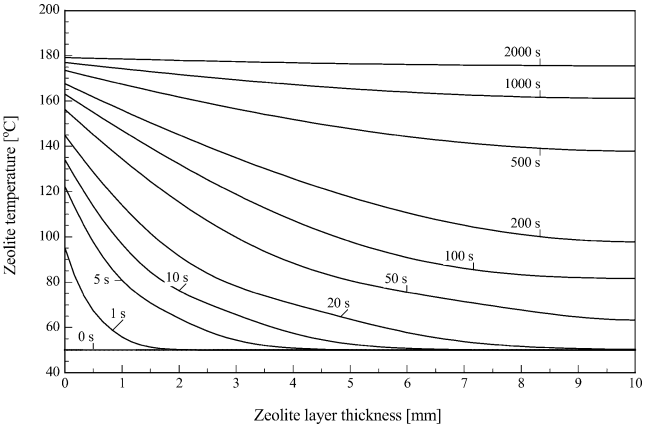

Fig. 8. Temperature distribution over the zeolite layer thickness during the desorption process.

gradient is shown in detail in Fig. 6 after 500 s. In other words, water is transferred from the bottom of the zeolite layer to the middle of it.

Fig. 6 shows also the further time variation of pressure distribution over the zeolite layer thickness during the rest of the adsorption process. Near the top of the layer, the pressure decreases sharply from 160 s to 200 s due to the fast decrease in temperature during this time (see Fig. 3). This results in a high pressure gradient, and consequently an increase in the rate of adsorption. This explains the jump in the uptake distribution near the top of the zeolite layer between 160 s and 200 s depicted in Fig. 5 as well as that between 200 s and 500 s in Fig. 7. This high rate of adsorption, which consequently means a high uptake, results, once more, in a decrease in the pressure gradient near the top of the layer after 500 s, which is to be taken from Fig. 6. After this time, the pressure gradient decreases gradually until the end of the adsorption process.

The movement of the adsorbed water from near the wall to the middle of the zeolite layer lasts, as shown in Fig. 7, until 6000 s. After this time, and due to the propagation of the uptake wave from the top of the layer, the uptake begins to increase once more near the wall. After 11460 s, the relative water uptake reaches the value of 95% and the adsorption process is terminated.

7.3. Desorption process

7.3.1. Temperature distribution

The time variation of the temperature distribution over the considered zeolite layer in the last section for the given parameters, initial and boundary conditions given in Table 3, is shown in Fig. 8. Due to the sudden increase of the wall temperature, the temperature of the lowest zeolite sub-layer increases sharply within the first second to 95 °C. After 100 s, it reaches 163 °C. On the other hand, the temperature of the highest sub-layer starts to increase after 20 s. The temperature over the zeolite layer thickness reaches nearly its final distribution after 2000 s.

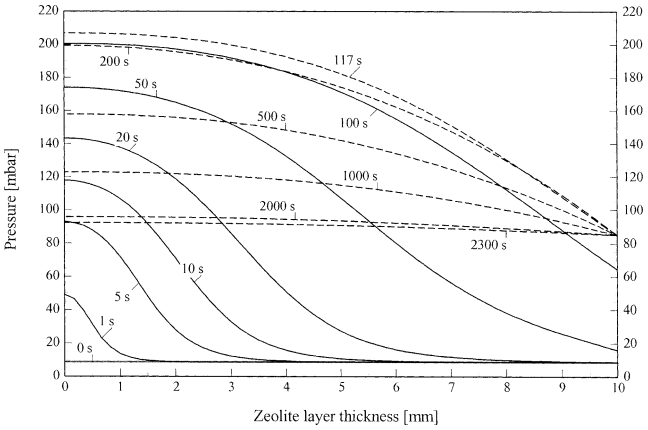

Fig. 9. Pressure distribution within the zeolite layer during the desorption process.

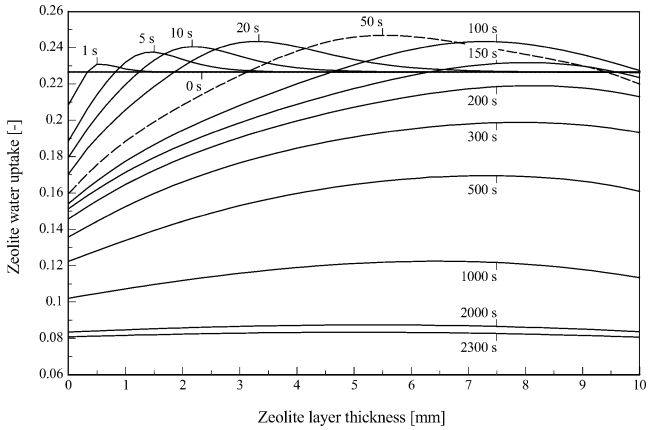

Fig. 10. Uptake distribution during the desorption process.

7.3.2. *Pressure and uptake distributions*

The pressure and uptake distributions during the desorption process are shown in Figs. 9 and 10, respectively. During the first 20 s, the equilibrium vapor pressure within the lowest sub-layer reaches 144 mbar, while that at the outermost sub-layer remains unchanged.

Simultaneously, and as shown in Fig. 10, the uptake reduction at the lower-most sub-layer is compensated by an uptake increase in the middle of the zeolite layer. This implies that, during this time interval, the adsorbed water near the heat exchanger wall migrates to the middle of the zeolite layer, while that in the middle migrates, in turn, to the top of the layer, without effectively desorbing any water to the vapor phase. After 50 s, the propagated uptake wave reaches the top of the layer and shows its impact by reducing the uptake under that at the beginning of the desorption process. The next presented uptake wave, after 100 s, shows once more an increase in the uptake at the top of the layer. This could be explained as a result of the accumulation of the internally desorbed water near the top of the layer up to this time instant.

After 117 s, as shown in Fig. 9, the pressure at the outermost sub-layer reaches the condenser pressure of 85 mbar, which means the end of the pre-heating phase. After this time instant, the condenser non-return valve is opened (see Fig. 1). Due to a proper condenser design, this condenser pressure is assumed to be held constant for the rest of the desorption process. In the mean while, the pressure at the lower-most sub-layer has reached its maximum value of 207 mbar. This indicates, that the maximum driving force to the considered desorption process is reached after 117 s. After this time instant, both pressure and uptake decrease gradually with time. After 2300 s, the relative water uptake reaches the value of 5%, and the desorption process is to be terminated.

7.4. *Effect of zeolite layer thickness*

Table 4 gives the effect of zeolite layer thickness on the duration of both adsorption and desorption processes discussed in Section 6. Comparing Figs. 6 and 9 reveals that the pressure gradients during the adsorption phase are clearly smaller than those during the desorption phase. The pressure gradient at the end of the pre-cooling phase, or in other words at the beginning of the adsorption phase, amounts to 8.5 mbar (see Fig. 6). After finishing the pre-heating phase, the desorption phase begins with a pressure gradient of about 120 mbar (see Fig. 9). As these pressure gradients are the main driving forces for both adsorption and desorption processes, the duration of the adsorption process is about 5 to 1.8 times that of the desorption process depending on the thickness of the zeolite layer. Reducing the layer thickness by 50% results in reducing the duration of the adsorption process to about 25% and that of the desorption process to 33%. As the heat gain, which can be coupled from the considered heat pump process at the considered operating conditions is constant, the power density of the adsorption heat pump process is inversely proportional to the cycle time. This leads to the conclusion that in order to get reasonable power densities from an AHP using zeolite layers, the layer thickness must not exceed 2.5 mm.

Table 4
Effect of zeolite layer thickness on the duration of both adsorption and desorption processes

Zeolite layer thickness [mm]	Duration of adsorption process [s]	Duration of desorption process [s]
10	11460	2300
5	2890	665
2.5	740	214
1.25	197	76
0.625	56	30

7.5. Effect of the volume of the vapor phase of the adsorber/desorber heat exchanger

The volume of the vapor phase of the adsorber/desorber heat exchanger has its direct impact on the duration of both pre-cooling and pre-heating phases. This can be taken from Table 5 for two selected thicknesses of the zeolite layer, namely, 10 and 2.5 mm. The volume of the vapor phase has been changed from 10 to 0.01 liter for the considered zeolite mass of 42 g. The durations of both pre-cooling and pre-heating phases decrease with decreasing the volume of the vapor phase and attain asymptotically their minimum values, which depend on the zeolite layer thickness, at the volume of 0.01 liter. The duration of the pre-cooling phase attains, for example, the minimum values of 93 and 8.71 s for the layer thicknesses of 10 and 2.5 mm, respectively.

The volume of the vapor phase of the adsorber/desorber heat exchanger is directly proportional to the mass of water vapor contained in this volume according to the ideal gas behavior formulated by Eq. (14). During both pre-cooling and pre-heating phases, the vapor pressure within the adsorber/desorber has to be changed from the condenser to the evaporator pressure, and vice versa, respectively. This means that, during the pre-cooling phase, an amount of water vapor, which is directly proportional to the volume of the vapor phase, has to be adsorbed before the vapor pressure reaches the evaporator pressure and the actual adsorption process begins. This occurs also but in the opposite direction during the pre-heating phase. This implies that the adsorption process starts effectively with a higher water uptake and that the desorption process begins actually with a lower water uptake than those uptakes, which can be obtained if the volume of the vapor phase may ideally vanish. The real adsorption heat pump process will thus operate between those two actual uptakes. According to the analysis of Westerfeld [16], the coefficient of performance (COP) of the AHP-process is directly proportional to the difference between those two uptakes. The decrease in the effective water uptake difference, from the ideal one, is termed, accordingly, as the unavoidable losses of the COP due to the volume of the vapor phase. At the considered operating conditions of the AHP, these losses amount to 12% and 0.3% for the volumes of the vapor phase of 10 and 0.1 liter, respectively, and are not dependent on the thickness of the zeolite layer. This means that the volume of the vapor phase of the adsorber/desorber heat exchanger of the AHP has to be minimized in order to minimize such unavoidable losses of the COP. The volume of the vapor phase of the adsorber/desorber heat exchanger must not exceed 2 liters per kg of zeolite in order to keep these unavoidable losses of coefficient of performance under 0.3%.

Table 5
Effect of the volume of the vapor phase of adsorber/desorber heat exchanger on the duration of both adsorption and desorption processes at two different thicknesses of the zeolite layer

Zeolite layer thickness	Volume of vapor phase	Duration of adsorption process [s]		Duration of desorption process [s]	
[mm]	[l]	Pre-cooling	Total	Pre-heating	Total
10	10	160	11460	117	2297
	5	125	11570	94.36	2298.33
	2	105	11643	79.62	2298.98
	1	99	11670	74.17	2299.24
	0.5	96	11683	71.26	2299.43
	0.1	94	11686	68.81	2299.52
	0.01	93	11697	68.23	2299.59
2.5	10	13.83	736.7	12.31	211.68
	5	11.24	745.2	9.98	211.79
	2	9.72	750.7	8.50	211.84
	1	9.22	752.7	7.97	211.87
	0.5	8.96	753.7	7.69	211.89
	0.1	8.76	754.6	7.46	211.91
	0.01	8.71	754.8	7.41	211.92

Decreasing the volume of the vapor phase results also in a very slight increase in the duration of the total adsorption as well as desorption processes. This is remarkable during the adsorption process with a volume of the vapor phase of 10 liter and a thickness of the zeolite layer of 10 mm, where the duration of the process is quite long. This can be explained by the increase in the effective water vapor uptake difference, which has to be adsorbed under the conditions of small pressure gradient (see Fig. 6), with decreasing the volume of the vapor phase.

8. Conclusions

A one-dimensional model for the combined heat and mass transfer during the adsorption/desorption of water vapor into/from a zeolite layer of an adsorption heat pump has been presented. The model is utilized to study the dynamics of both adsorption and desorption processes as well as to examine the influences of both the layer thickness and the volume of the vapor phase of the adsorber/desorber heat exchanger on these dynamics. The model equations have been numerically solved using the software packet gPROMS, which has proved itself as a powerful tool for modeling and simulating such a dynamic adsorption heat pump process.

The duration of the adsorption process is found to be 5 to 1.8 times that of the desorption process, depending on the zeolite layer thickness. Reducing the layer thickness by 50% results in a reduction to 25% in the duration of the adsorption process and to about 33% of the desorption process. In order to get reasonable power densities from an AHP using zeolite layers, the layer thickness must not exceed 2.5 mm.

The volume of the vapor phase of the adsorber/desorber heat exchanger has to be minimized, in order to minimize the unavoidable losses of the coefficient of performance of the adsorption heat pump during both the pre-cooling and the pre-heating phases. These results have to be considered for designing the adsorber/desorber heat exchanger of an adsorption heat pump.

References

[1] Process System Enterprise Ltd, http://www.psenterprise.com/gPROMS.
[2] D.M. Ruthven, Principles of Adsorption and Adsorption Processes, Wiley, New York, 1984.
[3] W. Kast, Adsorption aus der Gasphase; Ingenierwissenschaftliche Grundlagen und tecnische Verfaheren, VCH-Verlagsgesellschaft mbH, 1988.
[4] S. Eichengrün, E.R.F. Winter, Zeolith/Wasser-Adsorptionskälteanlage, Ki Luft- und Kältetechnik 3 (1994).
[5] D. Jung, N. Khelifa, E. Lävenmann, R. Sizmann, Energy Storage in Zeolites and Application to Heating and Air-Conditioning, Elsevier Science, Amsterdam, 1985.
[6] G. Restuccia, V. Recupero, G. Cacciola, M. Rothmeyer, Zeolite heat pump for domestic heating, Energy 13 (1988).
[7] Zhi Zhang Li, Wang Ling, Performance estimation of an adsorption cooling system for automobile waste heat recovery, Appl. Thermal Engrg. 12 (12) (1997) 1127–1139.
[8] J. Völkl, Heat conduction in zeolite beds, in: Proc. 7. Internat. Heat Transfer Conference, Munich, Germany, 1982, pp. 105–107.
[9] R. Lang, Leistungsfähige Adsorptionsmodule für eine Zeolith–Wasser–Wärmepumpe, Ph.D. Thesis, Aachen University of Technology (RWTH-Aachen), Germany, 1994.
[10] F. Bosnjakovic, K.F. Knoche, Technische Thermodynamic—Teil 2, 6th edn., Steinkopf Verlag, Darmstadt, Germany, 1997.
[11] B. Dawoud, Thermische und Kalorische Stoffdaten des Stoffsystems Zeolith MgNaA-Wasser, Ph.D. Thesis, Aachen University of Technology (RWTH-Aachen), Germany, 1999.
[12] U. Busweiler, W. Kast, Nichtisotherme Ad- und Desorptionskinetik am Beispiel der Wasserdampfadsorption an Einzelkörnen technischer Adsorbentien, Chem. Ing. Tech. MS-1284 (1984) 1–47.
[13] W. Krückels, Berechnung der Kinetik der Wasserdampfadsorption in mikroporösen hydratisierten Gelen, Habilitationsschrift, University of Stuttgart, Germany, 1973.
[14] F. Jokisch, Über den Stofftransport im hygroskopischen Feuchtebereich kapillarporöser Stoffe am Beispiel des Wasserdampftransports in technischen Adsorbentien, Ph.D. Thesis, Technical University of Darmstadt, 1975.
[15] R. Strauss, K. Schallenberg, K.F. Knoche, Measurement of kinetics of water vapour adsorption into zeolite layers, in: Symp. Proc. Solid Sorption Refrigeration, Paris, 18–20 November, 1992, pp. 227–231.
[16] T. Westerfeld, Numerische Untersuchung einer periodisch arbeitenden Adsorptions-wärmepumpe, Ph.D. Thesis, Aachen University of Technology (RWTH-Aachen), Germany, 1996.
[17] Min Oh, Modelling and simulation of combined lumped and distributed processes, Ph.D. Thesis, Dept. of Chemical Engineering and Chemical Technology, Imperial College of Science, Technology and Medicine, London, 1995.